5th Brazilian Conference on Composite Materials – BCCM 5
São Carlos School of Engineering – University of São Paulo
18th – 22nd January, 2021
V. Tita, J. R. Tarpani and M. L. Ribeiro (Editors)

THERMAL CONDUCTION MODELLING OF COMPOSITES BY EMBEDDING TECHNIQUE

Rafael Corrêa Salomão, Rogério Carrazedo

Department of Structural Engineering, São Carlos School of Engineering, University of São Paulo
Avenida Trabalhador São Carlense, 400, São Carlos, 13566-590, Brazil
rafaelsalomao@usp.br, rogcarrazedo@sc.usp.br

Keywords: Composite modelling, FEM, Embedding technique, Thermal problem

Abstract. *Composite materials are extremely important in several industrial areas and have been thoroughly used to solve many engineering problems. In more recent years, new numerical models and manufacturing processes have promoted a new interest spike on those materials. This work contributes to the state of the art of composite materials modelling by proposing an embedding technique for thermal problems using the finite element method. The technique relies on rewriting the reinforcement finite element variables according to the matrix finite element form functions. By doing such operations, it is possible to embed the reinforcement element without increasing the total degrees of freedom number. The embedding method is capable of modelling the phase's direction as well as it's placement. It's also possible to make use of non-linear conductive parameters to model non-linear thermal problems. Numerical examples are described to show the technique's capability. The numerical results show good agreement, as well as limiting an increase on the total number of degrees of freedom and being able to model nonlinear material behavior. Such characteristics make the model suitable to perform more complex analysis such as reliability, optimization, multi-physics, etc.*

1. INTRODUCTION

Composite materials are extremely important in several industrial areas and they are used to solve many engineering problems [1–2]. New numerical models and manufacturing processes have brought challenges to overcome. In this sense, this work proposes an embedding technique for thermal problems using the finite element method.

Composite material models are basely classified in three categories, according to its simulation technique: discretization, homogenization and embedding [3]. The embedding model used in this work has been successfully applied on structural models [4–5]. We now show the use of the same embedding strategy in thermal problems. The technique relies on rewriting the embed reinforcement variables according to the matrix form functions. By doing such operations, the reinforcement is embedded without increasing the total degrees of freedom number. The embedding method is capable of modelling the phase's direction as well as its placement, thus better representing the problem in comparison with other homogenization methods. It's also possible to make use of non-linear conductive parameters to model non-linear thermal problems.

2. FORMULATION

A heat transfer conduction problem on a solid could be stated as [6]:

$$\int_{\Omega} \delta\theta_{,i} k_{ij} \theta_{,j} d\Omega + \int_{\Omega} \delta\theta \rho c_e \dot{\theta} d\Omega = \int_{\Gamma} \delta\theta n_i q_i d\Gamma \tag{1}$$

where k_{ij} is the thermal conductivity, ρ is the material density, c_e is the specific heat, $n_i q_i$ is the heat flux normal to the surface Γ and θ is the temperature.

The first term on Eq. (1) is the total thermal conductivity on a solid. It is also assumed, for the case of a composite material, that the solid's total thermal conductivity is the sum of its matrix, fibers and particles phases: $K^{total} = K^{matrix} + K^{fibers} + K^{particles}$. Fibers and particles are henceforth called inclusions. Thermal conductivity parcel of the inclusions ($K^{inclusion}$) is discretized by finite elements as:

$$\begin{aligned} \int_{\omega} \delta\theta_{,i} k_{ij}^{inclusion} \theta_{,j} d\omega &= \int_{\omega} \frac{\partial(\phi_s(\eta_\gamma)\delta\theta_s)}{\partial x_i} k_{ij}^{inclusion} \frac{\partial(\phi_z(\eta_\lambda)\theta_z)}{\partial x_j} d\omega \\ &= \int_{\omega} \delta\theta_s B_{si} k_{ij}^{inclusion} B_{zj} \theta_z d\omega = \delta\theta_s K_{sz}^{inclusion} \theta_z \end{aligned} \tag{2}$$

where ϕ_s and ϕ_z are the shape functions from nodes s and z of the inclusion finite element. θ_s and θ_z are the temperature values from nodes s and z. η_γ and η_λ are the integrations points for the numerical integration on the inclusion domain ω. B_{si} is a matrix formed by the derivatives of the inclusion's shape functions and $K_{sz}^{inclusion}$ is the thermal conductivity matrix of the inclusion finite element.

The equality $\theta_s = \phi_{sq}(\xi_\alpha^s)\theta_q$ is used to rewrite the temperature from a node s of the inclusion finite element in terms of the matrix finite element temperature and shape functions from nodes q. ξ_α^s is the adimensional coordinate from the matrix finite element domain that corresponds to the position of the node s. As such, the information pertaining to the inclusion's element conductivity can be simply added to the matrix thermal conductivity matrix. The inclusion's element thermal conductivity matrix then becomes:

$$\begin{aligned} \int_{\omega} \delta\theta_s B_{si} k_{ij}^{inclusion} B_{zj} \theta_z d\omega &= \phi_{sq}(\xi_\alpha^s)\delta\theta_q \int_{\omega} B_{si} k_{ij}^{inclusion} B_{zj} d\omega \; \phi_{zr}(\xi_\beta^z)\theta_r \\ &= \delta\theta_q \phi_{sq}(\xi_\alpha^s) K_{sz}^{inclusion} \phi_{zr}(\xi_\beta^z) \, \theta_r \end{aligned} \tag{3}$$

where $\phi_{sq}(\xi_\alpha^s)$ a matrix responsible for the expansion of the original conductivity matrix into another with degrees of freedom compatible with the composite matrix finite elements.

With the adoption of convenient degrees of freedom arrangement, this *spread matrix* can be constructed as a concatenation of the composite matrix shape functions evaluated at the integration points related to the location of the nodes from the inclusion finite elements:

$$\phi_{ij}(\xi_\alpha^u) = \begin{bmatrix} \phi_{kl}(\xi_\alpha^1) & \cdots & 0 \\ \vdots & \ddots & \vdots \\ 0 & \cdots & \phi_{mn}(\xi_\alpha^\Upsilon) \end{bmatrix} \text{ with} \qquad (4)$$

$$\phi_{mn}(\xi_\alpha^\Upsilon) = [\phi^1(\xi_\alpha^\Upsilon) \quad \cdots \quad \phi^N(\xi_\alpha^\Upsilon)]$$

where ξ_α^Υ is the adimensional coordinate on the matrix element that corresponds to the inclusion element node Υ and ϕ^N is the shape function from matrix element node N.

Finally, the resulting conductivity matrix for the expanded inclusion finite element (Eq. (5)) can be added directly to the global solid's thermal conductivity matrix, according to its degrees of freedom. As such, this embedding technique doesn't promote an increase on the total number of degrees of freedom.

$$[K^{inclusion}]_{global} = [\phi]^T [K^{inclusion}][\phi] \qquad (5)$$

3. NUMERICAL EXAMPLES

Some numerical examples are presented to show the embedding technique capability.

3.1. Single fiber reinforcement

The first example shows the inclusion of a single long fiber through a plate. The numerical results are compared with those obtained from software ABAQUS. The matrix is modeled by 244 triangular finite elements with cubic approximation. The embedded fiber is modeled by 20 linear elements with linear approximation. Boundary conditions and employed mesh are shown on Fig. 1. Notice that the nodes from the meshes of both matrix and fiber don't need to be coincident, as seen on Fig. 1b. Also, the inclusion of the fiber mesh doesn't increase the total degree of freedom number. The following properties are adopted: $k^{matrix} = 2.75\,W/m°C$, $k^{fiber} = 55\,W/m°C$ and $Area^{fiber} = 0.01m^2$.

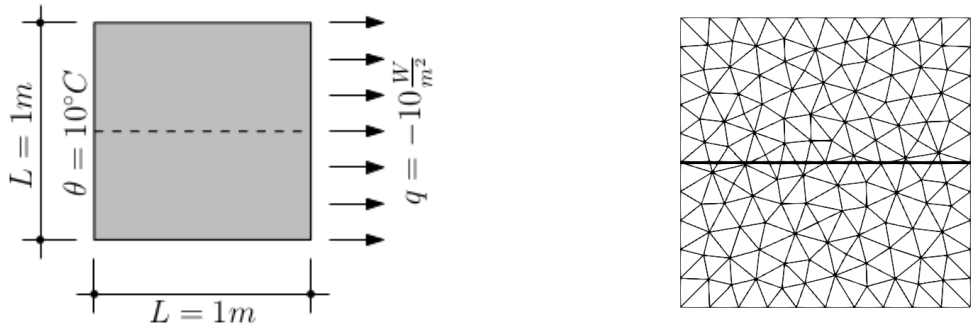

(a) (b)

Figure 1 – (a) Boundary conditions for the problem. (b) Mesh employed for the matrix and fiber.

Figure 2 shows the resulting thermal distribution, while Fig. 3 represents the temperature on the right border. Good agreement between both results is found.

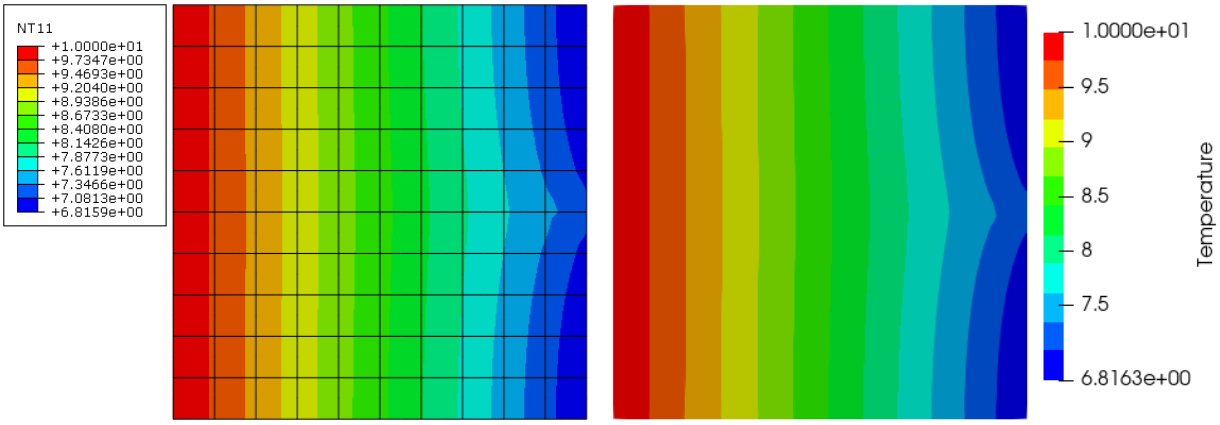

(a) (b)

Figure 2 – Temperature distribution of plate reinforced with one horizontal fiber. (a)ABAQUS. (b) Proposed technique.

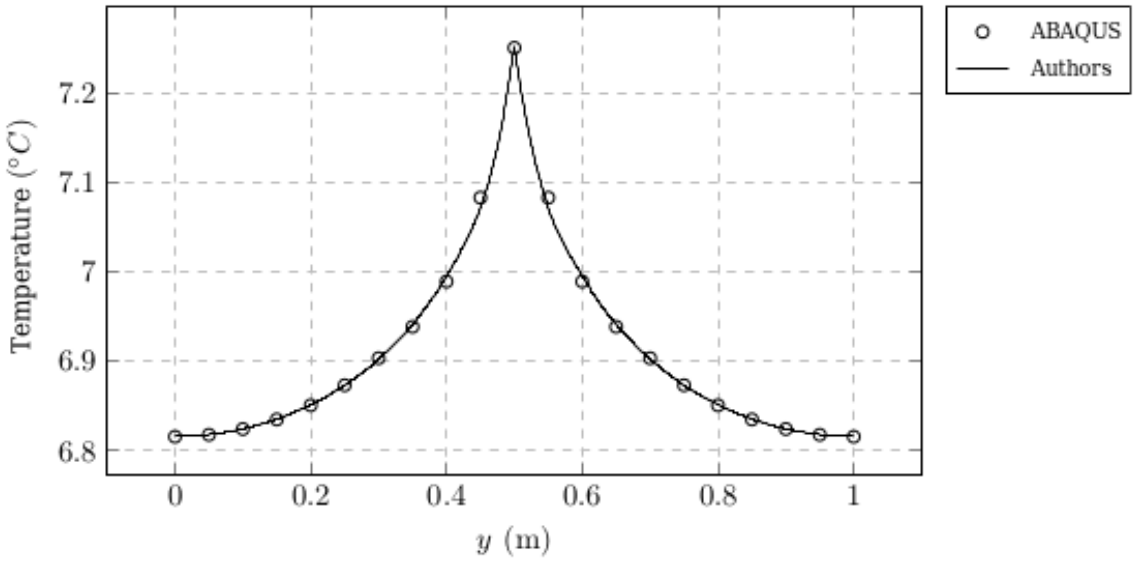

Figure 3 – Temperature distribution on the plate right edge.

3.2. Internal defect

In this second example, a concrete block with an internal defect is subjected to thermal loads, as shown in Fig. 4a, based in [7]. Fig. 4a also shows its boundary condition and dimensions. This problem was modeled as the composition of a matrix and a particle mesh of negative conductive parameter to account for the internal defect. For reference, the problem is also modeled by complete discretization of its phases, as shown in Fig. 4b.

The following properties were used: $k^{matrix} = 2.75\,W/m°C$, $k^{defect} = 0.6875\,W/m°C$, $k^{particles} = -2.0625\,W/m°C$, $h = 13.95\,W/m^2°C$ and $\theta_\infty = 0.0\,°C$.

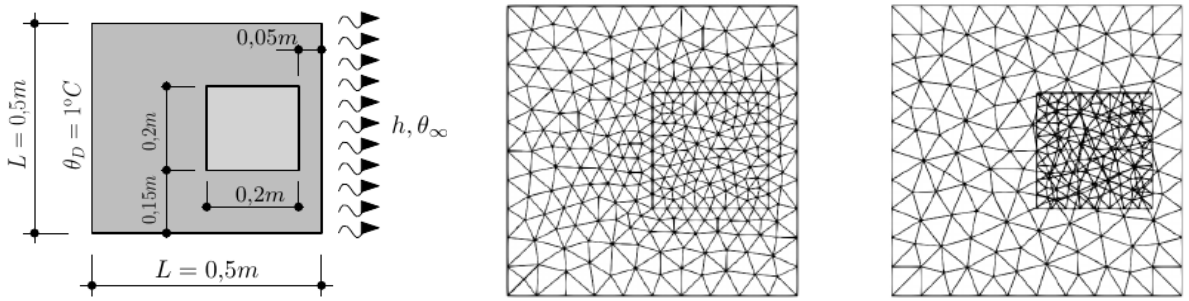

(a) (b) (c)

Figure 4 – Problem definition and finite element meshes (a) Problem definition; (b) FEM mesh for the reference; (c) FEM mesh for the embedded model.

Figure 5 shows the thermal distribution of both reference (Fig. 5a) and particle (Fig. 5b) mesh. It's possible to note the good agreement on the temperature results:

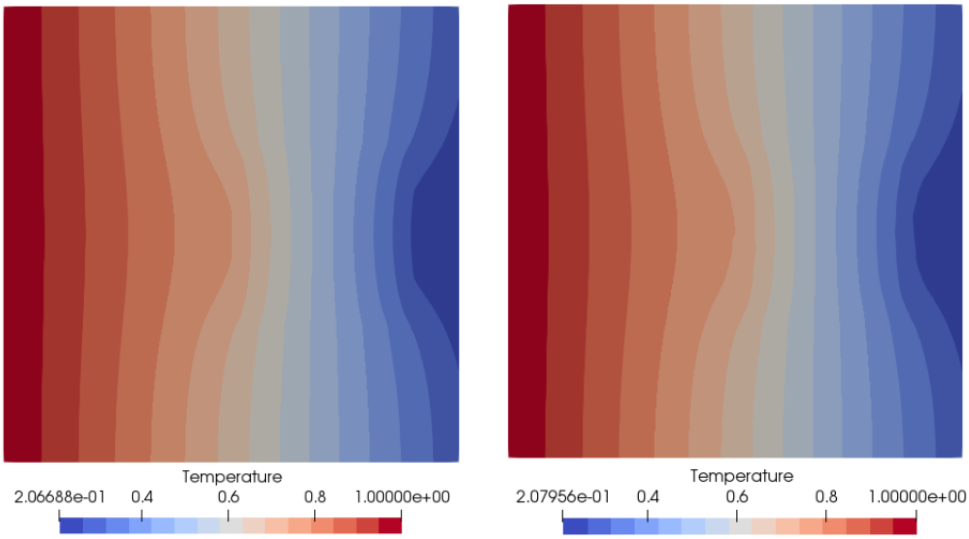

(a) (b)

Figure 5 – Temperature field obtained (a) reference problem; (b) embedded model.

Figure 6 shows the temperature on the right border. Again, it's possible to note very good agreement between the reference and embedded mesh results.

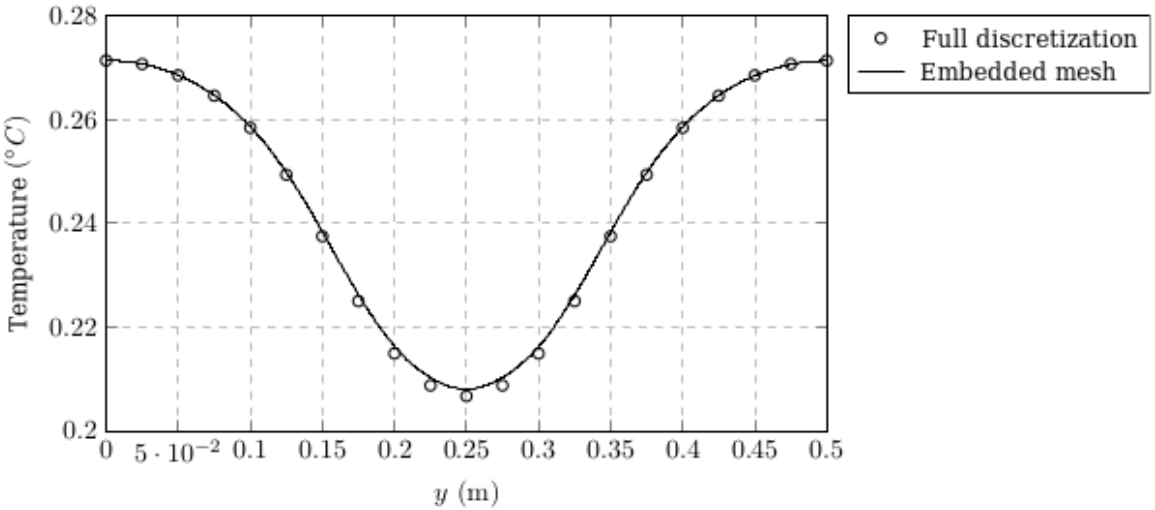

Figure 6 – Temperature along the plate's high for the right most edge.

3.3. Nonlinear fiber reinforced material

In this third example, we show that it is also possible to model nonlinear materials. This example considers two cases (with and without fiber reinforcement) as shown on Fig. 7a and 7b, where the corresponding dimensions and boundary conditions are also shown. Figures 7c and 7d show the respective meshes for the matrix and the fibers. 126 triangular elements with cubic approximation have been used to model the matrix, and 20 fibers, each one made of 10 linear elements, have been employed to model the reinforcement. The following thermal properties are: $k^{fiber} = 55\,W/m°C$, $Area^{fiber} = 0.0005\,m^2$ and $k^{matrix}(\theta) = 2.75 - 0.2\theta\,W/m°C$.

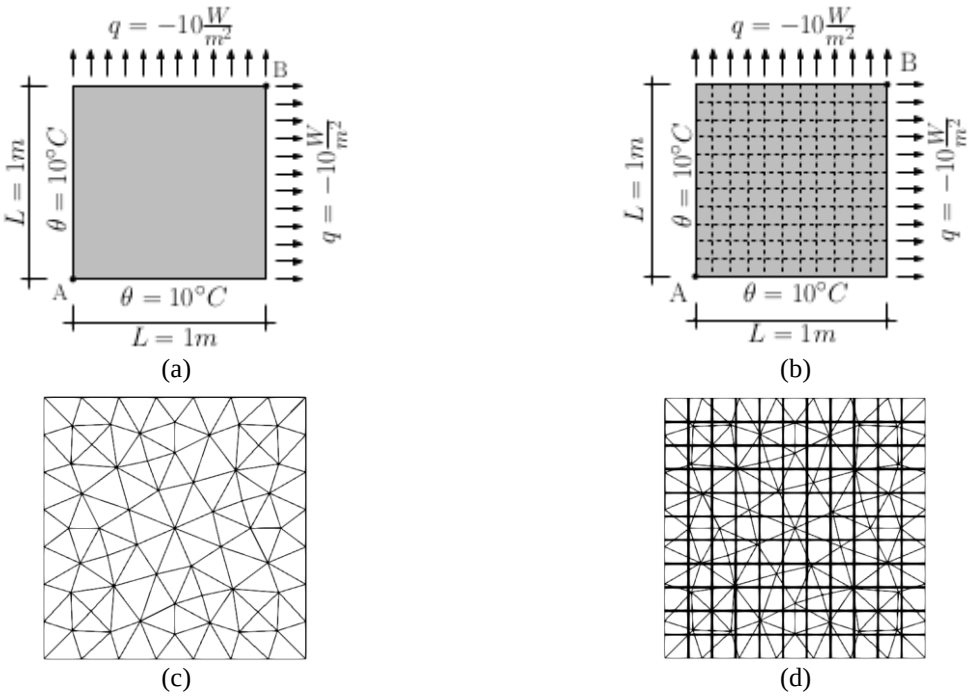

Figure 7 – (a) Boundary conditions and dimensions for the case without fiber reinforcement. (b) Boundary conditions and dimensions for the case with reinforcement (c) Mesh for the matrix (d) Mesh for the matrix and fibers from the reinforcement.

Figure 8 shows the temperature along a line segment defined by points A-B, see Fig. 7a. Notice that the model is capable of capturing the non-linear behavior of the matrix material. Considering only the nonlinear matrix material case (Fig. 8c), it's also possible to note that the model can capture the reinforcement effect on the composite.

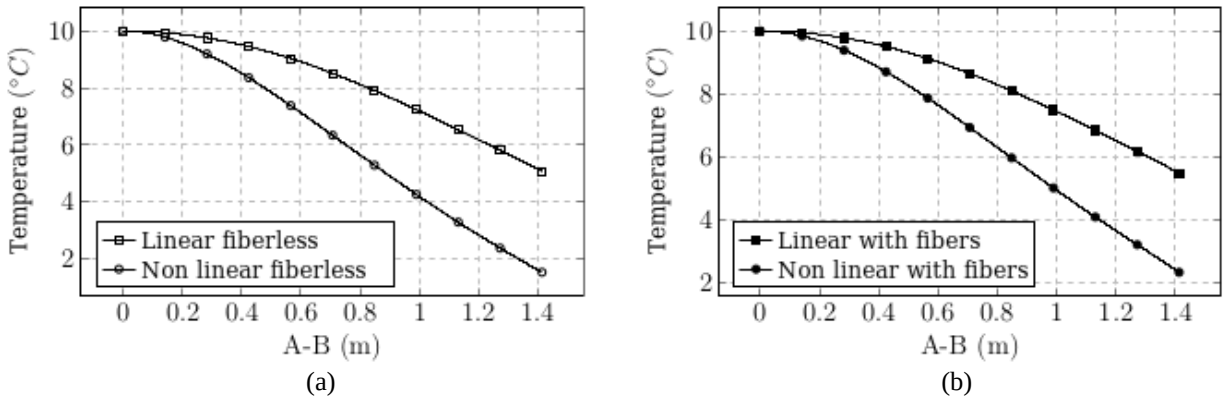

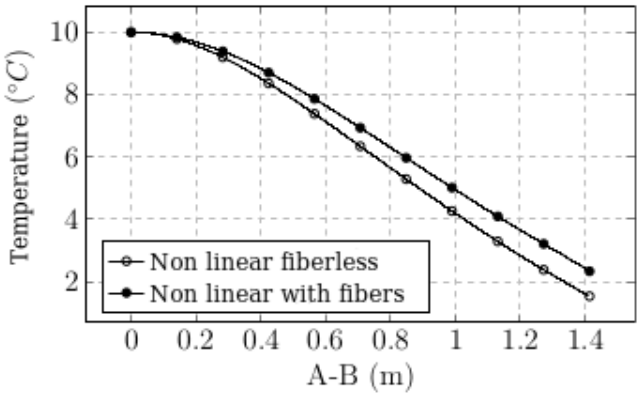

(c)

Figure 8 – Temperature distribution along the line segment A-B. (a) Linear and nonlinear results for the fiberless case. (b) Linear and nonlinear results for the cases with fibers. (c) Comparisons between the nonlinear cases.

4. CONCLUSION

The proposed embedding technique to model composite materials for thermal problems has significant advantages relative to other model strategies. The total number of degrees of freedom remain constant irrespective to the number of inclusions and both inclusion and matrix meshes are independent. It is also possible to make use of nonlinear conductive materials without any change to the model strategy. Coupled with a mechanical model that makes use of the same embedding technique, it's possible to solve thermomechanical problems without incurring in accuracy loss from information transfer between the mechanical and thermal fields.

ACKNOWLEDGEMENTS

This study was financed in part by the Coordenação de Aperfeiçoamento de Pessoal de Nível Superior - Brasil (CAPES) - Finance Code 001.

REFERENCES

[1] L. Linganiso; R. Anandjiwala. Fibre-reinforced laminates in aerospace engineering. *Advanced Composite Materials for Aerospace Engineering*, p. 101–127. (2016).
[2] X. Zhang; Y. Chen; J. Hu. Recent advances in the development of aerospace materials. *Progress in Aerospace Sciences*, p. 22–34. (2018).
[3] M. Azim et al. Energy Absorption Capacity of Reinforced Concrete Beam-Column Connections, with Ductility Classes Low. *American Journal of Civil Engineering and Architecture*, p. 42–52. (2014).
[4] R. R. Paccola; D. Piedade Neto; H. B. Coda. Geometrical non-linear analysis of fiber reinforced elastic solids considering debounding. *Composite Structures*, p. 343–357. (2015).
[5] R. R. Paccola; H. B. Coda. A direct FEM approach for particulate reinforced elastic solids. *Composite Structures*, p. 282–291. (2016).
[6] Lienhard, IV, J. H. and Lienhard, V, J. H. *A Heat Transfer Textbook*. Phlogiston Press. Cambridge, MA. 5th edition. (2019).
[7] Inacio, G. R. et al. *Análise de viabilidade do uso de termográfica como ensaio não-destrutivo para identificação de falhas internas de concretagem*. In: XXX CILAMCE - Congresso Ibero Latino Americano de Métodos Computacionais em Engenharia, Armação de Búzios. (2009).

RESPONSIBILITY NOTICE

The authors are the only responsible for the printed material included in this paper.